UNIVERSITY OF ROMA
TOR VERGATA

ENGINEERING SCIENCES COURSE
A.A. 2016/2017
Graduation thesis

EVALUATION OF THE RESIDENCE TIME DISTRIBUTION IN A SCREW REACTOR : THE AXIAL DISPERSION MODEL

SUPERVISOR

PROF. STEFANO CORDINER
PROF. VINCENZO MULONE

CANDIDATE

ANDREA DE MATTEIS

SUPERVISOR ASSISTANT

ENG. ALESSANDRO MANNI

Table of contents

Abstract

Biomasses thermochemical conversion may give a significant contribution to the flexible and programmable production of electric and thermal power in the context of renewable sources. In this perspective, the fast pyrolysis process is a very interesting technology whose role is rapidly increasing. Until now, only few models have been developed to describe screw reactor systems behavior designed for biomass fast pyrolysis. As happen in all the thermochemical processes, temperature profile play a crucial role, and in particular for fast pyrolysis purposes. Hence, a consistent heat transfer model is needed to develop a reliable simulation framework. Moreover, to be solved properly, the heat transfer model requires an advanced residence time description to be applied on the mass flow evolution along the reactor. The aim of this thesis is then the evaluation of this distribution by means of a previous 3D DEM numerical analysis data. This further evaluation will be done with an Axial Dispersion Model ADM. The ADM solution will be achieved by a numerical simulation with the method of lines: by spatial discretization, the problem is reduced into a series of Ordinary Differential Equations. The ODE system is then solved in MatLab environment.

1.Introduction

Over the last years, an increasingly demand of energy production has been observed worldwide. Due to the serious environmental challenges and energy shortage brought on by the massive consumption of fossil fuels, it has become a global consensus to develop renewable and sustainable energy [1, 2]. For that reasons, models involving energetic, environmental and economic issues, have been applied to support state policies able to reduce the impact of the excessive use of carbon in energy production [2]. The correlation between energy consumption, economic growth and energy induced emissions has shown the impact on environmental degradation of the increasing energy demand[3]. As a result, a deep research activity has started worldwide to support the utilization of renewable sources [4]such as bioenergy from thermochemical processes [5]. In this context, a peculiar aspect of renewable energy sources is related to their local character and their inherent diffused geographical availability. A distribution of the energy generation is therefore the objective toward which the development of the current energy source scenario is focused on [6]. the deployment of renewable energy technologies will contribute significantly to energy independence of all the regions in the world [7], with associated economic and environmental benefits [8-10]. However, the harvesting of renewable resources represents a very large component of cost associated with biomass energy production and generation. This cost is higher compared with the one of fossil fuels due to the huge difference in volumetric energy content [11]. As a consequence, the increase of energy density turns out to be of fundamental importance in the use of biomass as source of energy. One of the possible approaches is the intermediate conversion of solid biomass into liquid or gaseous products, through biochemical or thermochemical processes. However, the strong dependence of performance parameters from feedstock characteristics [12] and conversion technology design aspects[13], makes the design process and consequently whole system cost effectiveness challenging. Useful to this aim are the information collected from small to full scale experiments, such as those reported in literature available studies [14] for fixed bed[15, 16], microwave[17], fluidized[18, 19], entrained flow [20] and free fall reactors[21]. So in general the use of experimental data is a valuable tool to support design strategies. Modeling tools such as the numerical ones for wastes [22] and biomass conversion [23, 24] are of outmost importance as well. they are able, in fact, to describe processes like the torrefaction [25, 26] the gasification [27, 28],such as fixed bed systems[29, 30], and pyrolysis ones [31]. Furnaces fed by biomass residues [23, 24] have been deeply developed by this kind of approach as well. Same considerations may be made for the fast pyrolysis process which is rapidly increasing as a reliable solution, for residual materials such as biomasses [32] and wastes [33]. Numerous numerical fast pyrolysis models, focused on the improvement of bio-oil production parameters, have been developed and can be found in the literature [34-37]. Until now, very few models have been developed to describe a screw reactor system behavior designed for biomass fast pyrolysis and only recently ad hoc dimensional analysis for such a kind of systems has been proposed[38]. Continuous reactors, generally presents imperfect flow characteristics, which can led to variations in the desired residence time due to stratification or undesired back mixing. The non ideality produce a residence time distribution that describe in general the probability that a particle will spend

a certain amount of time in such conditions. Then, to properly model heat and mass transfer, the prediction of the residence time distribution is mandatory. From experimental measurements, it has been found that the time each particle spends inside the reactor has not a constant value, but it is different for each infinitesimal mass composing the flow rate. Consequently, since the length of the reactor has a fixed value, also the velocities of the different particles inside the reactor will assume different values. As a consequence, each of them will have its personal heating history and conversion rate. It is therefore fundamental to evaluate a velocity function in order to understand the different reactions that will occur inside the reactor for each considered particle. Two different directions can be taken to face with this problem. The first one is to define in each reactor section a fixed distribution from the inlet to the outlet. This distribution can be evaluated by simple analytical models or by experimental campaigns. However in this case, the considered distribution is just the one observed at the exit of the reactor. This hypothesis has a very strong impact on the results, since the particles history can dramatically affect the process evolution. Is in fact widely known that, depending on different system characteristics, a certain particle distribution will develop inside the reactor. The second direction assume that the particles distribution will evolve along the reactor together with the reactions. Therefore, some particles will be faster, some others will proceed with a lower velocity. The knowledge of such distribution evolution along the reactor, allow to better match experimental data with numerical results by a simultaneous RTD-heat and mass transfer coupling. In this work, data from 3D simulation have been considered to be compared with a simplified model output. This model, namely Axial Dispersion Model, can evaluate in a simplified manner such evolution by means of a convective diffusive equation evolving along the reactor.
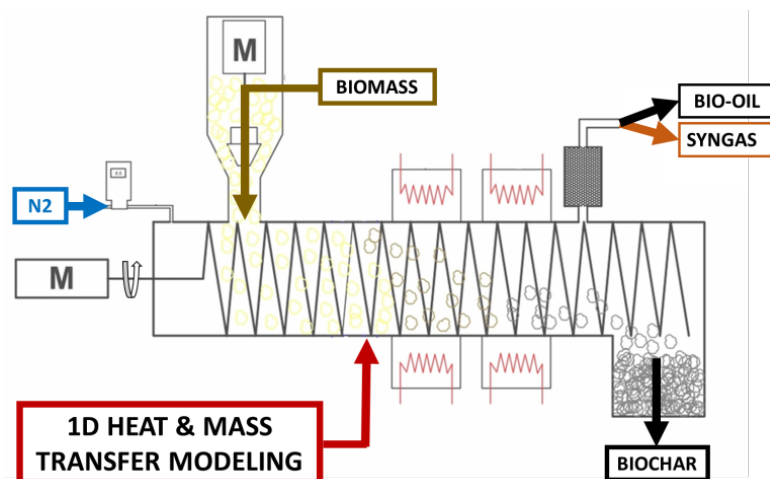
Figure 1: Overall system setup

Figure 1 shows the simplified model of the fast pyrolysis process. Pyrolysis in general means the rapid heating up in the absence of oxygen. Should be noted that, among the all possible technologies, fast pyrolysis has been chosen for the increasing interest in producing biofuels technologies. The high oil conversion is, in fact, the most attractive characteristic of this process. The thermal reactions transform biomass to biochar , oil and/or gases . All these products can be used without further processing to provide heat or power. Moreover, the pyrolysis oil can be converted to high-quality liquid fuels via bio-refinery processes.

2.The Residence Time Distribution

In chemical engineering, the correct processing of a certain specie in a specific reactor, does not depend only the average parameters, but on their time and spatial distribution as well. In a rotary drum, the same consideration can be analogously done: the process yield is strictly connected to such distribution. This spread is caused by secondary patterns in the flow above the average field. The particles in the reactor are in fact subject to two main mechanisms that cause them to move.
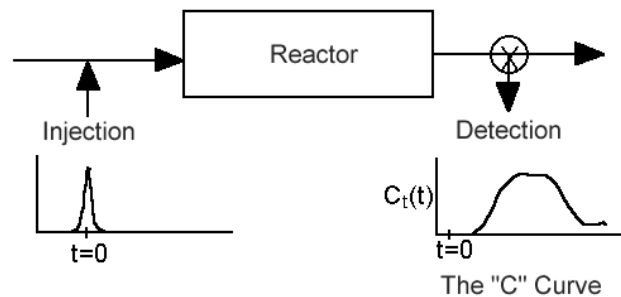

Figure 2: RTD injection and detection [39]

The first one is an overall convection which moves the bulk from inlet to outlet with a global axial velocity equal to the mean value of the velocity profile. The second mechanism happens on a smaller scale and will generate axial dispersions of the individual particles or rather conglomerates of particles. These secondary movements have velocity components in both the longitudinal (axial) and transverse direction. Due to their random behavior, the secondary movements can be mathematically described by a diffusion coefficient (for fluid systems) or dispersion coefficient (for solid systems). All these mechanisms have a certain influence upon the time spent by the particles in the reactor. Therefore, the knowledge of the RTD is of paramount importance in the reactor design since it can dramatically affect its reaction performance. This fact occur since the RTD describes the probability that a certain particle or chemical species will spend a specific time at desired reaction conditions. Take as example a continuous reactor with a sharp, low-variance RTD. The mean residence time value at the target reaction time is favorable for translating from bench-scale batch reactor conditions. This will allow more precise control of reaction extent and ultimately the ability to maximize desired intermediate product yield.

2.1 RTD modeling

To date, many studies have been done on developing different models to simulate and evaluate the RTD in rotating reactors. This because it is a crucial index in understanding the material flow profile. As a consequence, such evaluation is widely used in many industrial processes, such as the continuous manufacturing of chemicals, plastics, polymers, food, catalysts, and pharmaceutical products. In order to achieve satisfactory output from a specific unit operation, raw materials are designed to stay inside the unit under specific operating conditions for a specified period of time. This residence time information is usually compared with the time necessary to complete the reaction or process within the same unit operation. For example, the local reaction rate coupled with the time the mass stays inside the reactor determines the unit performance. If the time

required to complete the reaction is longer than the actual residence time, the process cannot provide a complete operation and fails its design purpose.

The research on the RTD in chemical engineering fields focused on Different points of view. From the influence of operation conditions, materials, and the unit geometry on the RTD profile, to the improvement of measurement and modeling methods for different processes and units. Due to the wide scope of the RTD issue, many papers have been published concerning different applications[40, 41]. Therefore, the RTD can be evaluated with the use of different models that will be here presented. Moreover, one of them will be chosen for the thesis specific case.

2.1.1 CSTR and PFR series

Modern RTD theory, has been originally developed from continuous fluid systems. Early fluid reactor models assumed plug flow in a tubular-shape reactor (PFR), or perfect mixing in continuous stirred tank reactors (CSTR). These conceptions represent two extreme RTD profiles in the reactor. In real case continuous flow systems, experimental RTD profiles are usually between the two extremes. Combinations of CSTR and PFR are then used in modeling practical cases. CSTR in a series model is one commonly used model:

$$\tau = \frac{NV_0}{F} \tag{2.1}$$

$$E(\theta) = \frac{N(N\theta)^{N-1}}{(N-1)!} e^{-N\theta} \tag{2.2}$$

Where τ is the mean residence time (MRT), N the number of CSTR tanks, V_0 the volume of each tank, and F the volumetric flow rate. $E(\theta)$ represents the dimensionless RTD and $\theta = t/\tau$ the dimensionless time. This model is a one-parameter model, so that the idealness of the RTD is represented by the number of CSTR tanks used. Large number of tanks indicates a PFR-like reactor, and a small number leads to a CSTR-like reactor.

2.1.2 Axial dispersion model

Despite the combination of CSTR and PFR elements, the axial dispersion model is an efficient alternative to generalize the RTD concept to most non-ideal reactors. The PDE representing the axial dispersion process of a tracer in the flow system, or the Fokker–Planck equation (FPE), is a simple 1D equation.

$$\frac{\partial c}{\partial t} = D_{ax} \frac{\partial^2 c}{\partial x^2} - u_s \frac{\partial}{\partial x} c \tag{2.3}$$

The explanation of the different parameters composing equation (2.3) together with its formulation will be considered later on since this is the model chosen for the evaluation of the RTD.

A mention should be made on the most widely used solution of the Fokker-Planck equation, developed by Taylor with open-open boundaries:

$$E(\theta) = \frac{1}{2\sqrt{\pi\theta/Pe}} e^{[-\frac{Pe(1-\theta)^2}{4\theta}]} \tag{2.4}$$

This solution expresses the Residence Time Distribution function taking as only

independent parameter the dimensionless time $\theta = t/\tau$. τ is the mean residence time (MRT); $Pe = u_s l/D_{ax}$ represents the Peclet number, and l is the distance between injection and detection points. This solution was applied in the fitting of experimental RTD data in various systems and good agreement was obtained, especially for rise-delayed or long-tailed RTD profiles, showing the robustness of the Taylor's dispersion model.

Despite its reliability, the Taylor's dispersion model gives the residence time distribution function just at the exit of the reactor. However, for the purpose of this thesis, interest is given to a more general solution that is able to solve the ADM also in the interior points $(x/l < 1)$. For this reason, no further considerations will be made about the Taylor solution.

2.1.3 Stochastic model

Another widely used RTD model, consider the particle movement as a stochastic process. In particular the axial motion of any particle or small fraction of material inside a continuous system, is considered as a two dimensional probabilistic process. As a result, the overall RTD curve can be calculated by the accumulation of the random axial motions of these small fractions. An example of stochastic model that is similar to the CSTR and PFR series, is the Markov chain model. Briefly, this model arbitrarily defines the ratio of flux exchange among assumed elements connected in a network. This is done considering that the successive system state depends only on the current one and nothing else. Although the exchange of flux is well modelled among different elements, mixing inside each element is not considered in a Markov chain model. This fact differ this case from the CSTR and PFR series model. It is important to note that this model is very useful when the flow regions within the system can be easily distinguished into different elements. As an example granular flows with heterogeneous cross-wise layers.

2.1.4 Bimodal RTD

Bimodal RTD profile results from two or more main flow components traveling differently, for instance, through two paths in reactor, or on different layers in a granular flow system. The dual peaks result from the overlap of RTD components through different paths. Those kind of systems are not common, therefore they are not deeply considered in literature. In fact, due to case-sensitivity, no quantitative models have been developed for bimodal RTD profile until now. However, the Bimodal RTD will probably be useful in a future development aimed at the study of particular components that would turn out to have a bimodal behavior.

2.1.5 Convolution

In considering fluid systems, it is common to have a non-ideal tracer injection due to a relatively short MRT compared to the injection period of a fluid pulse. The algorithm of convolution, introduced by Danckwerts, has been applied in recent studies since the injection was usually not a perfect pulse. In the case considered in this thesis, the MRT is much higher than the injection period, so that this model will not be considered for our purposes.

2.2 Model Selection: coupling with heat and mass transfer

As already mentioned, the model chosen for the evaluation of the RTD is the Axial Dispersion Model ADM. The main reason behind this choice lies in the possibility of computing a velocity distribution inside the reactor. This distribution, after a resampling into an arbitrary chosen number of values, can be then directly inserted into a complete heat and mass transfer model [42]. A stiff system of differential equations will be defined and then solved using Matlab. Moreover, the ADM gives advantages under a computational point of view since it can be solved by means of a finite difference approximation of the PDE describing the model. This will lead to a sequence of time distributions (of number equal to the number of lines) that describe not only the distribution at the exit of the reactor, but also inside its length. To better understand the framework where this thesis project will be inserted, the energy transfer modeling of the fast pyrolysis process will be here briefly presented.

The process of heat transfer represents for sure the most important aspect for the fast pyrolysis reactor design. Screw conveyors have unique features in terms of heat transfer characteristics, which can be shared with rotary kilns. As a consequence, the same approach used in the mathematical modeling of heat transfer in a rotary kiln Thermo-Reactor has been used. The screw velocity in fact, similarly to kilns rotation speed, has a strong influence on heat transfer coefficients especially between the wall and the solid bed. In Figure 3, the schematic of a control volume is given.
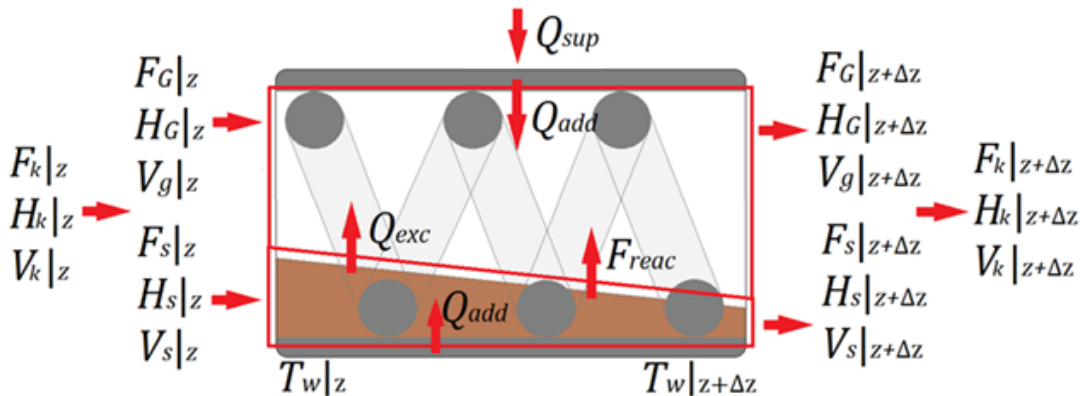

Figure 3: Model control volume

The model [42]has been developed considering some assumptions as solid and gas phases well mixed over the radial direction, variable solid particle size, gas phase behaving as a perfect gas and finite axial dispersion. According to Figure 3, the mass flow rate of the individual species is considered. Chemical reaction described by the reaction rate k_k will influence the flow rate F_k. The steady state mass balance over the control volume can be evaluated for the single species as reported in table 1. Individual velocities V_k have been evaluated [43] according to the experimental RTD simulation from a 3-D DEM approach. The gaseous fraction velocity can be derived from the total area expression (table 1). The total mass conservation is ensured by the differential form (DF) of the total area. Concerning the energy balance equations, the above considered is a multiphase system. It consists therefore of two domains with two coupled energy balance equations: one for the solid phase and one for the gaseous phase. From table 1, a global formulation of the energy balance equation over the entire control volume can be

evaluated. The first term LHS represents the heat of reactions. From the global formulation, the energy balance for both the solid and gaseous phase can be evaluated in two similar ways as reported in table 1. In the solid phase equation, $\dot{q}_{a-ul,s}$ is the sum of unit length conductive and radiative heat fluxes from wall to solid bed, and $\dot{q}_{e-ul}$ the sum of convective and radiative fluxes exchanged with the gas phase. Concerning the energy balance over the gaseous phase, $\dot{q}_{a-ul,g}$ represents the unit length heat flux given by the exposed wall to the gas phase through convection and radiation, and $\dot{q}_{e-ul}$ the convective flux exchanged with the solid phase.

The problem gives a $[17n_v + 4] \times [17n_v + 4]$ system. In this system, n_v is the number of sub-velocities given by the resampling of the velocity distribution obtained from the solution of the ADM. The number of n_v can be decided arbitrarly by extracting the required amount of velocity values from the RTD analysis. In this way, the ADM solution can be inserted into the more general pyrolyzer solution in the heat and mass transfer model. In fact, after having provided the initial conditions at z=0, the set of equations commented above, are solved in MatLab by means of the ode15s solver (step size must be taken extremely small to avoid instability in the solution). However, Definition of heat transfer fluxes are required to solve the ODE set. This has been done in [42] as follow: in such a reactor, as reported in Figure 4, the thermal energy externally provided, is given to the solid bed and to the gas phase via two different paths: one across the exposed bed surface and the other one through the covered bed surface. At the exposed surface, the solid phase absorbs heat by convection and radiation, while the covered bed region gets heat mostly via conduction at the wall.
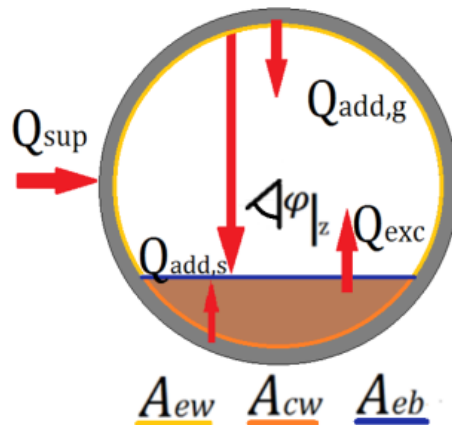

Figure 4: Heat transfer model diagram

Again, due to similarities between screw conveyors system and rotary kiln ones, heat transfer coefficients have been determined [44, 45]. Description of the heat transfer model can be done with the use of an equivalent electric circuit. In this kind of approach, electrical resistances are represented by terms as $1/h_k A_k$ and voltage generators are used to substitute the gas, solid and wall temperatures. As a consequence, the heat transfer per unit length can be evaluated from the equations reported in table 1. Thermal resistance will be constituted of a term which depends on the solid contact [46] and another one related to the gas film at the surfaces interface. Thus, the conductive heat transfer coefficient between the covered wall and the covered bed can be evaluated (table 1). As already highlighted, the convective heat transfer is made of two terms: Q_{ew-g}^{cv} and

Q_{eb-g}^{cv}. They express respectively the heat transfer between the gas phase and the exposed wall and bed surface. Convective coefficients can be evaluated by means of the equations proposed in [47] for a rotary kiln and reported in table 1. The radiative heat transfer has been modelled under the following main assumptions: bodies are considered grey, the axial temperature gradient is negligible, the view factors are taken constant and equal to unity, emissivity and transmissivity are assumed constant over the reactor length abscissa.

Table 1: Model equations

| Balance equations	
Mass Balance	$$\sum_{i=1}^{n_v} \frac{\partial F_{w,i}}{\partial z} + \frac{\partial F_{m,i}}{\partial z} + \sum_{j=1}^{3} \frac{\partial F_{vb,j,i}}{\partial z} + \frac{\partial F_{ab,j,i}}{\partial z} + \frac{\partial F_{c,j,i}}{\partial z} + \frac{\partial F_{g,j,i}}{\partial z} + \frac{\partial F_{t,j,i}}{\partial z} + \sum_{k=1}^{n} \pm \frac{k_k F_k}{V_k} = 0$$
Total area constancy	$$\sum_{k=1}^{n} A_k = \sum_{k=1}^{n} \frac{F_k}{\rho_k V_k} = cost. = \pi R^2$$
Total area constancy D.F.	$$\frac{\partial}{\partial z}\left(\frac{F_N}{\rho_N V_g}\right) + \sum_{i=1}^{n_v} \frac{\partial}{\partial z}\left(\frac{F_{w,i}}{\rho_w V_i} + \frac{F_{m,i}}{\rho_m V_g}\right) + \sum_{j=1}^{3} \frac{\partial}{\partial z}\left(\frac{F_{vb,j,i}}{\rho_b V_i} + \frac{F_{ab,j,i}}{\rho_b V_i} + \frac{F_{c,j,i}}{\rho_c V_i} + \frac{F_{g,j,i}}{\rho_g V_g} + \frac{F_{t,j,i}}{\rho_t V_g}\right) = 0$$
Energy balance	$$\sum_{k=1}^{n} \frac{k_k F_{k,z}}{V_k} \Delta H_k + \sum_{k=1}^{n} F_k C_{pk} \frac{\partial T_k}{\partial z} = \dot{q}_{a-ul}$$
Energy balance over solid bed	$$\left[\sum_{i=1}^{n_v} F_{w,i}C_{pw} + \sum_{j=1}^{3} F_{vb,j,i}C_{pb} + F_{ab,j,i}C_{pb} + F_{c,j,i}C_{pc}\right]\frac{\partial T_s}{\partial z}$$ $$= -\left[\sum_{i=1}^{n_v} \frac{F_{w,i}k_m}{V_i}\Delta H_m + \sum_{j=1}^{3} \frac{F_{ab,j,i}k_{2,j}}{V_i}\Delta H_2 + \frac{F_{ab,j,i}k_{3,j}}{V_i}\Delta H_3\right] + \dot{q}_{a-ul,s} + \dot{q}_{e-ul}$$
Energy balance over gaseous phase	$$\left[F_N C_{pN} + \sum_{i=1}^{n_v} F_{m,i}C_{pm} + \sum_{j=1}^{3} F_{g,j,i}C_{pg} + F_{t,j,i}C_{pt}\right]\frac{\partial T_g}{\partial z} + \left[\sum_{i=1}^{n_v} \frac{\partial F_{m,i}}{\partial z}C_{pm} + \sum_{j=1}^{3} \frac{\partial F_{g,j,i}}{\partial z}C_{pg} + \frac{\partial F_{t,j,i}}{\partial z}C_{pt}\right](T_g - T_s)$$ $$= -\sum_{i=1}^{n_v}\sum_{j=1}^{3} \frac{F_{t,j,i}k_4}{V_g}\Delta H_4 + \dot{q}_{a-ul,g} - \dot{q}_{e-ul}$$
Heat transfer model equations	
wall to bed	$$\dot{q}_{a-ul,s} = \left(h_{cw-cb}^{cd}A_{cw} + h_{ew-eb}^{r}A_{eb}\right)(T_w - T_s)$$
exchanged	$$\dot{q}_{e-ul} = -(h_{eb-g}^{cv} + h_{eb-g}^{r})A_{eb}(T_s - T_g)$$
wall to gas	$$\dot{q}_{a-ul,g} = (h_{ew-g}^{cv} + h_{ew-g}^{r})A_{ew}(T_w - T_g)$$
Conductive and convective coefficients	
Covered.wall.-covered bed	$$h_{cw-cb}^{cd} = \frac{1}{\left(\chi\frac{D_p}{k_g}\right) + \left(2\sqrt{\frac{[(1-y)k_b\rho_b C_{pb} + yk_c\rho_c C_{pc}]\cdot n \cdot \sin\alpha\cos\alpha}{pitch}}\right)^{-1}}$$
Exp. wall-gas	$$h_{ew-g}^{cv} = \left(1.54Re_g^{0.575}Re_s^{-0.292}\right)\frac{k_g}{D_e}$$
Exp. bed-gas	$$h_{eb-g}^{cv} = \left(0.46Re_g^{0.535}Re_s^{0.341}\eta^{-0.341}\right)\frac{k_g}{D_e}$$
Radiative coefficient	
Exp. wall- bed	$$h_{ew-eb}^{r} = \frac{(J_w - J_s)(\tau_g F_{eb-ew})}{T_w - T_s}$$
Exp. bed-gas	$$h_{eb-g}^{r} = \frac{(J_s - E_g)(\epsilon_g F_{eb-g})}{T_s - T_g}$$
Exp. wall-gas	$$h_{ew-g}^{r} = \frac{(J_w - E_g)(\epsilon_g F_{ew-g})}{T_w - T_g}$$

2.3 RTD measurement in rotary kiln

The distribution of residence times can be examined by injecting inert material (tracer) into the reactor. The tracer can be then analyzed in concentration at the reactor exit in order to evaluate the RTD. In literature, two methods of tracer injection, called respectively pulse tracer and step tracer, are mostly considered. In case of pulse tracer method, an amount of tracer is instantaneously injected in one or more shots to the feed stream of the reactor in a very short time. Subsequently the tracer concentration is measured as a function of time and the RTD can be obtained. Differently, the step tracer method uses a constant rate of tracer injection during the measurement. Clearly, RTD measurements from the two methods are different; it is important to specify that, however, the responses from the two methods are related to each other and the pulse response is readily translated into the step response, and vice-versa.

In this thesis, the pulse tracer injection methodology has been used. In the MatLab simulation, this translates in a row vector representing the tracer injection at the initial time. The tracer distribution is represented by a step function of unitary height and width decided by experimental activity considerations. This means that, after the discretization of the spatial coordinate, the tracer will have its amplitude over an l number of lines. This number l can either be arbitrarily decided or can be set as a percentage of the number of lines. The latter solution is desirable in the case of a great amount of lines in order to have the resultant 3-D plot of the tracer distribution in proportion with the discretized spatial coordinate.

Nevertheless, it is important to note that the width of the tracer injection is not a parameter which influences the overall result of the experiment and that the RTD can be successfully studied by selecting a default value for l. In fact, the pulse response curve will always be a Gaussian one as can be seen from figure 5.
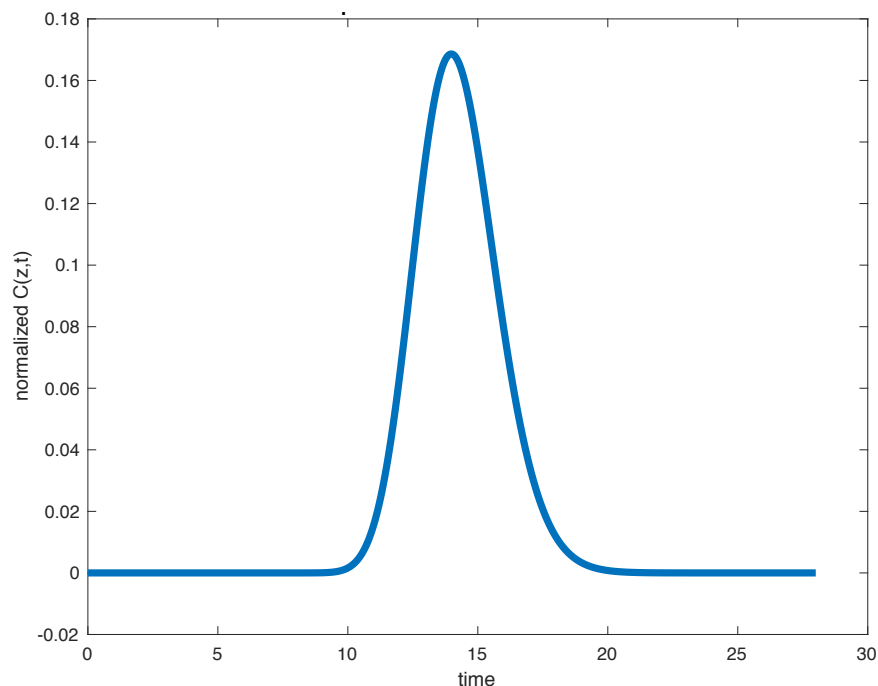
Figure 5: plot of the exit concentration
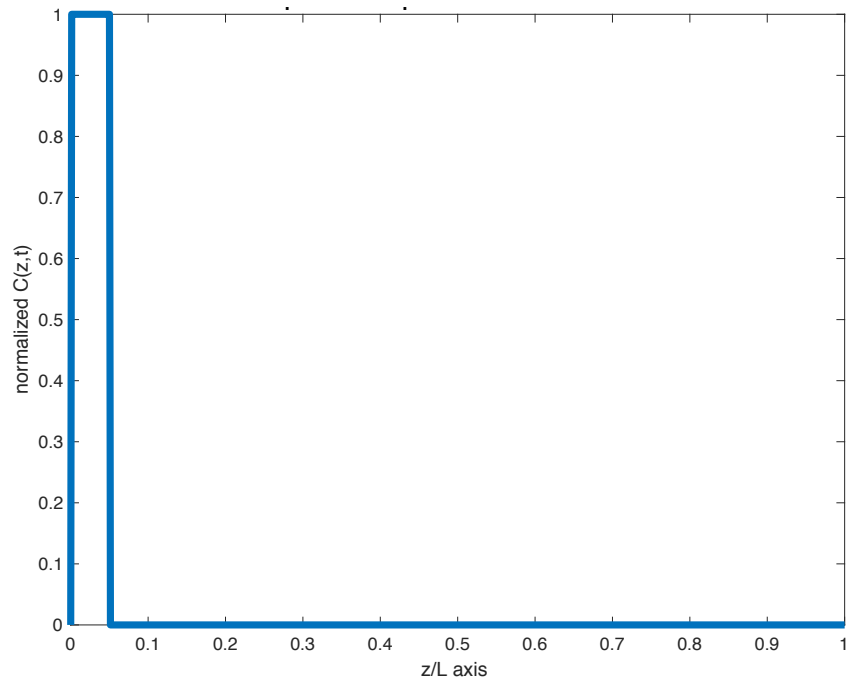
Figure 6: plot of the input tracer concentration

3. Axial dispersion model

In this thesis, the axial dispersion of tubular reactor was employed to describe behavior of the flow in the reactor, i.e. residence time distribution. The following derivation, follows the one reported in [48]. The model structure comes from an unflighted rotary kiln with length L and diameter D, which is fed by a continuous solid mass flow rate m_s. These hypotheses are used for the derivation of the axial dispersion model (ADM).
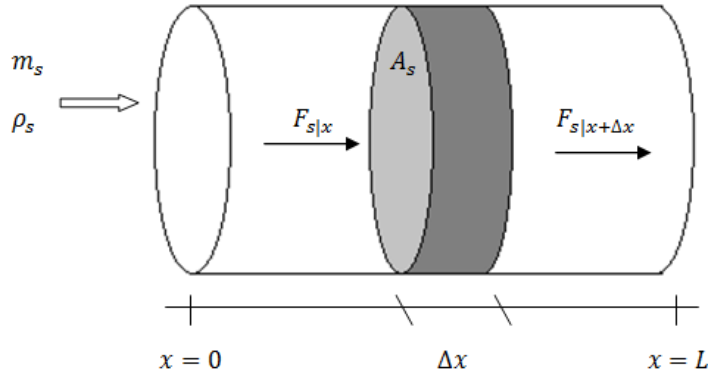

Figure 7: Model of the unflight rotary kiln

In particular, a differential element Δx in the reactor is considered. The mass balance of sold flow over element Δx without reaction is given as:

Now – Before= In – Out

$$\Delta x A_s \rho_s \big|_{x,t+\Delta t} - \Delta x A_s \rho_s \big|_{x,t} = \Delta t F_s \big|_{x,t} - \Delta t F_s \big|_{x+\Delta x,t} \tag{3.1}$$

Dividing equation (3.1) by $\Delta x \, \Delta t$, and taking the limit Δx, $\Delta t \rightarrow 0$ the equation will become

$$\frac{A_s \rho_s \big|_{x,t+\Delta t} - A_s \rho_s \big|_{x,t}}{\Delta t} = \frac{\Delta t F_s \big|_{x,t} - \Delta t F_s \big|_{x+\Delta x,t}}{\Delta x} \tag{3.2}$$

$$\frac{\partial}{\partial t} (A_s \rho_s) = -\frac{\partial F_s}{\partial x} \tag{3.3}$$

From Flick's law of diffusion, mass flow rate (F_s) is written as:

$$F_s = u_s A_s \rho_s - D_{ax} \frac{\partial}{\partial x} (A_s \rho_s) \tag{3.4}$$

Where u_s, A_s, ρ_s, and D_{ax} are the solid velocity (m/s), cross-sectional area of the bed (m^2), bulk density of solid bed (kg/m^3), and axial dispersion coefficient (m/s), respectively. By substitution of Equation (3.4) into equation (3.3), will be

$$\frac{\partial}{\partial t} (A_s \rho_s) = \frac{\partial}{\partial x} \left(D_{ax} \frac{\partial}{\partial x} (A_s \rho_s) \right) - \frac{\partial}{\partial x} (u_s A_s \rho_s) \tag{3.5}$$

The bulk density of the solid bed (ρ_s) will be considered as constant within the model, and the equation will become

$$\frac{\partial A_s}{\partial t} = \frac{\partial}{\partial x} \left(D_{ax} \frac{\partial A_s}{\partial x} \right) - \frac{\partial}{\partial x} (u_s A_s) \tag{3.6}$$

Equation (3.6) is essentially a relation to describe the bed cross section area $A_s(t,z)$ in time and space.

In order to develop a model to compute the RTD of solid, tracer mass fraction, x_t, is introduced into equation (3.6), and the final form of the axial dispersion equation is given as

$$\frac{\partial c}{\partial t} = \frac{\partial}{\partial x}\left(D_{ax}\frac{\partial c}{\partial x}\right) - \frac{\partial}{\partial x}(u_s c) \tag{3.7}$$

Where $c = x_t A_s$ is proportional to the amount of tracer.

Equation (3.7) is a Partial Differential Equation known as the Fokker-Planck Equation (FPE). This equation will be later on discretized into a set of n Ordinary Differential Equations (being n the number of lines) to be solved using the ODE15s Matlab stiff integrator. n initial conditions $(t = 0)$ are therefore needed, one for every ODE. This has been done using a step function of unitary height inserted inside the Matlab code through a vector of one line and n columns. The vector will be composed by all zeroes except for a number l of columns whose values will be set equal to 1.

In this analysis, the dispersion coefficient, as well as the solid velocity, are considered space independent. Therefore the equation becomes:

$$\frac{\partial c}{\partial t} = D_{ax}\frac{\partial^2 c}{\partial x^2} - u_s\frac{\partial}{\partial x}c \tag{3.8}$$

As already stated in chapter 2, lots of studies have been done about Residence Time Distribution and different models can be used to describe it. In this thesis the ADM has been chosen for the evaluation. One of the reasons lies in the clear physical meaning of the parameters in the Fokker Planck Equation: u_s and D_{ax} indicates the combination of the convective axial transport and the superimposed axial dispersion. The axial dispersion coefficient is a function of the solid velocity u_s, the length of the reactor (L) and the Axial Peclet number Pe_{ax}

$$D_{ax} = \frac{u_s L}{Pe_{ax}} \tag{3.9}$$

This equation is very useful in understanding the dependence of the axial distribution on the convective over diffusive ratio by means of the axial Peclet number evaluation.

3.1 RTD Evaluation

The RTD is usually described by the age distribution of a material in an extruder $E(t)$: this quantity is called *residence-time distribution function.* This function is obtained as a result at the exit of the reactor to our pulse tracer injected at the beginning of the simulation. In this way $E(t)$ can be defined as:

$$E(t) = \frac{C(t)}{\int_0^\infty C(t)dt} \tag{3.10}$$

Where $C(t)$ is the concentration, or mass fraction of tracer that leaves the reactor at time t. With respect to equation (3.7), $C(t)$ corresponds to $c(t,z)$ evaluated at $z = L$.

Another parameter which usually is taken to describe the RTD is the exit age over time $F(t)$. This curve is interrelated to the $E(t)$ curve and it represents the cumulative distribution function in the exit stream at any time. It is given by

$$F(t) = \int_0^t E(t)dt \cong \frac{\sum_0^t C(t)\Delta t_i}{\sum_0^\infty C(t)\Delta t_i} \tag{3.11}$$

Application of mean residence time (τ) and its variance (σ^2) are also important parameters of RTD. The particle mean residence time, is defined by the following mathematical expression:

$$\tau = \int_0^\infty tE(t)dt = \frac{\int_0^\infty C(t)tdt}{\int_0^\infty C(t)dt} \tag{3.12}$$

The variance, which represents the square of the spread of distribution, is calculated by the following equation:

$$\sigma^2 = \int_0^\infty (t - \tau)^2 E(t)dt \tag{3.13}$$

From the above discussion, it can be seen that the fundamental computation in studying the RTD in a screw reactor is the evaluation of the Residence Time Distribution function. In fact, evaluation of the other parameters comes directly from numerical computation of $E(t)$. Moreover, the evaluation of the function E will connect this thesis with the study of reactor energy and mass balances previously seen. In fact, that study takes as input $E(v)$ that is, the RTD function expressed in function of the average travelling velocity of the particular concentration inside the reactor. Therefore, the main objective will be the computation of the Residence Time Distribution function.

4. Axial Dispersion Model: the method of lines

According to chapter 3, the axial dispersion model, which was developed to calculate the residence-time distribution of granular solid within rotary kiln, is a partial-differential equation (PDE) in space and time derivative. The producing of analytical results is very complex and requires too much time. Therefore, numerical solution is the better choice to solve the model of axial dispersion. Ideally, the numerical solution is simply a numerical evaluation of the analytical solution. But since an analytical solution is generally unavailable for realistic PDE problems in science and engineering, the numerical solution is an approximation to the analytical solution and our expectation is that it represents the analytical solution with good accuracy. The method of lines (MOL) is a general procedure for the solution of time dependent PDEs and it is the one that has been chosen in this thesis. This solution has been considered also because the method of lines has been used to make the energy balance of the process happening in the pyrolyzer. Thus, the use of the same procedure to solve also the problem of the RTD allows to include the two codes in the same template in order to have a complete and unique model to simulate the fast pyrolysis process.

The basic idea of the MOL is to replace the spatial derivatives in the PDE with algebraic approximations[41]. Once this is done, the spatial derivatives are no longer stated explicitly in terms of the spatial independent variables. Thus, only the physical initial conditions are needed. In other words, a system of ODEs that approximate the original PDE has been obtained with only one remaining independent variable. The challenge, then, is to formulate the approximating system of ODEs. Once this is done, any integration algorithm for initial value ODEs can be used to compute an approximate numerical solution to the PDE. In this thesis, the Matlab stiff integrator ODE15s has been considered.

In the illustration of the MOL, an alternative notation for PDEs is considered. Instead of writing the partial derivatives as in equation (3.8), it is more convenient to use a *subscript notation* that is easier to state and allows a more direct association with computer coding. For instance, equation (3.8) can be written as

$$c_t = D_{ax}c_{xx} - u_s c_x \qquad (4.1)$$

Where, c_t is a subscript notation for $\partial c / \partial t$. In other words, a partial derivative is represented as the dependent variable with a subscript that defines the independent variable. For n order derivatives, the independent variable is repeated n times, for example, c_{xx} represents $\partial^2 c / \partial x^2$.

To apply the MOL to equation (4.1), the algebraic approximations of c_x and c_{xx} are needed. Their *finite difference approximations (FD)* are therefore considered.

$$c_x \approx \frac{c_i - c_{i+1}}{\Delta x} \qquad (4.2)$$

$$c_{xx} \approx \frac{c_{i-1} - 2c_i + c_{i+1}}{\Delta x^2} \qquad (4.3)$$

where i is an index defining a position along the grid in x, and Δx is the spacing in x along the grid, assumed constant. Thus, for the left end value of x, $i = 1$, and for the right end value of x, $i = n$, i.e., the grid in x has n points. Then the MOL approximation of equation (3.8) is:

$$\frac{\partial c_i}{\partial t} = D_{ax} \frac{c_{i-1} - 2c_i + c_{i+1}}{\Delta x^2} - u_s \frac{c_i - c_{i+1}}{\Delta x} \qquad 1 \leq i \leq n \tag{4.4}$$

The equation (4.4) is written as an ODE since there is only one independent variable, t. What it has just been obtained is a system of n ODEs. This transformation of a PDE to a system of ODEs, illustrates the essence of the MOL, namely, the replacement of the spatial derivatives, so that the solution of a system of ODEs approximates the solution of the original PDE. Then, to compute the solution of the PDE, we compute a solution to the approximating system of ODEs.

4.1 Initial and Boundary conditions

Before considering this integration in t, we have to complete the specification of the PDE problem. Equation (3.8) is second order in x and first order in t, so it requires one initial condition and two boundary conditions. This comes directly from the number of auxiliary conditions needed to solve a PDE problem. This is determined by the highest derivative order in each independent variable. Since eq. (3.8) is first order in t and second order in x, it requires one auxiliary condition in t and two auxiliary conditions in x. The t is termed an initial value variable and therefore requires one initial condition (IC). It is an initial value variable since it starts at an initial value, t_0, and moves forward over a finite interval $t_0 \leq t \leq t_f$ without any additional conditions being imposed.

Since x is termed a boundary value variable, therefore requires two boundary conditions (BCs). It is a boundary value variable since it varies over a finite interval $x_0 \leq x \leq x_f$, and at two different values of x, conditions are imposed on c in equation (3.8). Typically, the two values of x correspond to boundaries of a physical system, and hence the name boundary conditions.

In our problem, ICs are expressed as

$$c(x, t = 0) = A(x) \tag{4.5}$$

Since equation (4.4) constitute n initial value ODEs, n initial conditions are required. These will be

$$c(x_i, t = 0) = A(x_i) \qquad 1 \leq i \leq n \tag{4.6}$$

$A(x)$ is a vector of n elements.

Concerning the Boundary Conditions, the Danckwerts boundary conditions are used, namely

$$c(x = 0, t) = 0 \tag{4.7}$$

$$\frac{\partial c(x = x_f, t)}{\partial x} = c_x\big(x = x_f, t\big) = 0 \tag{4.8}$$

Equations (4.7) and (4.8) applies at the two extremes of the space domain. This means that, after the discretization of the domain into n lines, they are applied to the first and last one. Therefore, for $i = 1$ we will have

$$\frac{\partial c}{\partial t} = c_t = 0 \tag{4.9}$$

since the value of $c(x = 0, t) = 0$ does not change after being set as an initial condition. On the other side, for $i = n$, from the discretization of equation (4.8)

$$\frac{c_i - c_{i+1}}{\Delta x} = 0 \Rightarrow c_i = c_{i+1} \tag{4.10}$$

After having set the IC and BCs, and after having obtained the discretized form of our ADM, we can pass to the numerical solution of the model and, finally, to the calculation of the RTD parameters.

5. Matlab code

In the following, a MatLab code in which the previous method has been implemented, is presented and commented.

This purpose, is achieved with a main program that requires as input the number of lines and the initial conditions ICs. Moreover various plots and checks are included in the program. A second code part is then considered for the specification of some problem parameters and for the definition of the FD approximation of eq. (3.8). Boundary conditions BCs are then specified. The MatLab stiff integrator ODE15s is considered for the computations.

After the ADM solution, focus is placed on the evaluation of the RTD. This is done in the main template with the addition of some code lines which take as input results obtained from the above mentioned procedure. Finally, the evaluation of the velocity distribution inside the reactor, together with its resampled form, is programmed.

5.1 Numerical solution of the Axial Dispersion Model

The main Matlab template used to solve the Axial Dispersion Model, is listed below:

```matlab
% file pde_main
clear all
  clc

l=40;
n=input('numero di linee');
x=1;
A(1)=0
for i=1:n
   if i<l+2 && i>1
       A(i)=x
   else A(i)=0
   end
end


  for i=1:n
      c0(i)=A(i)
  end

  t0=0.0;
  tf=24;
  tout=linspace(t0,tf,n);
  nout=n;
  ncall=0;

  reltol=1.0e-10; abstol=1.0e-10;
  options=odeset('RelTol',reltol,'AbsTol',abstol);
```

```matlab
[t,c]=ode15s(@pde_1_diffusion_convection_final,tout,c0,options)

        % A 3D plot is also produced
figure(2);
colormap('Gray');
C=ones(n/10);
g=linspace(0,1,n); % For distance x
tmp=downsample(c,10);
U=downsample(tmp.',10).';
t=downsample(t,10);
g=downsample(g,10);
h1 = surface(t,g,U',C);
axis('tight');
grid off
xlabel('time [s]')
ylabel('z/L axis ')
zlabel('normalized V(z,t)')
s1 = sprintf('Fokker Plank Equation - MOL Solution');
sTmp = sprintf('u(x,0) = sin(\\pi x/2 )');
title([[49]], 'fontsize', 12);
rotate3d on;

% check
ingresso=0;
for index=1:n
    ingresso=c(1,index)*(1/n)+ingresso;
end

uscita=0;
for index=1:n
    uscita=c(240, index)*(1/n)+uscita;
end
error=((input-exit)/((input+exit)/2))*100
```

The following points about the main program are here presented:

After clearing the workspace and the command window, the user is asked to specify the number of lines n to apply the MOL. The Initial Conditions (for $t = 0$) are built over an n point grid in x by means of a row vector representing the amount of tracer initially injected in the reactor. The vector is composed by all zeroes except for a number of columns decided by the template (in the considered case, *l=40*) that will have the value specified by the variable x. The result is a vector which simulates, as already stated, a step function representing the tracer injected in the reactor.

```matlab
% the number of lines is asked
n=input('numero di linee');

% Initial condition is computed over an n point grid in x
l=40;
x=1;
A(1)=0
for i=1:n
   if i<l+2 && i>1
       A(i)=x
   else A(i)=0
   end
end


  for i=1:n
      c0(i)=A(i)
  end
```

The independent variable t for the ODE integration is defined

```matlab
t0=0.0;
  tf=24;
  tout=linspace(t0,tf,n);
  nout=n;
  ncall=0;
```

The n ODEs are integrated by a call to the Matlab stiff integrator ode15s. This integrates the system of differential equations $c' = f(t, c)$ from t_0 to t_f with initial conditions c_0. Each row in the solution array c corresponds to a value returned in column vector t. With options, some integration settings are considered. They are the absolute and relative error tolerances that allow a more precise integration.

```matlab
reltol=1.0e-10; abstol=1.0e-10;
  options=odeset('RelTol',reltol,'AbsTol',abstol);
  [t,c]=ode15s(@pde_1_diffusion_convection_final,tout,c0,options)
```

A 3-D plot is also produced

```matlab
 figure(2);
  colormap('Gray');
  C=ones(n/10);
  g=linspace(0,1,n); % For distance x
  tmp=downsample(c,10);
  U=downsample(tmp.',10).';
  t=downsample(t,10);
```

```
g=downsample(g,10);
h1 = waterfall (t,g,U',C);
axis('tight');
grid off
xlabel('time [s]')
ylabel('z/L axis ')
zlabel('normalized V(z,t)')
s1 = sprintf('Fokker Plank Equation - MOL Solution');
title([[40, 49-54]], 'fontsize', 12);
rotate3d on;
```

A comparison between the amount of injected tracer and the amount of tracer observed at a specific time instant is made by calculating the area of the step function at $t = 0$ and the area of the curve that is present at that instant.

```
input=0;
for index=1:n
    input=c(1,index)*(1/n)+input;
end

exit=0;
for index=1:n
    exit=c(240, index)*(1/n)+exit;
end
error=((input-exit)/((input+exit)/2))*100
```

The ODE solution by ode15s is evaluated by calling a function defined in a sub-routine. This will specify the n ODEs obtained after the discretization of the PDE that will be solved by the stiff integrator ODE15s.

```
% File: pde_1_diffusion_convection_final.m

function ct=pde_1_diffusion_convection_final(t,c)

  global ncall
  xl=0.0;
  xu=0.25;
  n=length(c);
  dx2=((xu-xl)/(n-1))^2;
  dx=((xu-xl)/(n-1));
  us=0.0206;
  d=0.00001;

  for i=1:n
```

```matlab
   if(i==1)      ct(i)=0;
   elseif(i==n) ct(i)=d*(c(i-1)-c(i))/dx2;
   else
               dcdx=(c(i+1)-c(i))/dx
               dcdx2=(c(i-1)-2*c(i)+c(i+1))/dx2;
               ct(i)=d*dcdx2-us*dcdx;



   end
 end
 ct=ct';
 ncall=ncall+1;
```

Some considerations can be made about this function as well: firstly some problem parameters are defined.

```matlab
 global ncall
  xl=0.0;
  xu=0.25;
```

The defining statement at the beginning of the sub-routine indicates that the indipendent variable t and dependent variable vector c are the i inputs of the function. The obtained output is the vector of t derivatives, ct (where $ct = \partial c/\partial t$). This means that all of the n ODE derivatives in t are defined.

The finite difference of eq. (3.8) is then programmed.

```matlab
 n=length(c);
 dx2=((xu-xl)/(n-1))^2;
 dx=((xu-xl)/(n-1));
 us=0.0206;
 d=0.00001;

 for i=1:n

   if(i==1)      ct(i)=0;
   elseif(i==n) ct(i)=d*(c(i-1)-c(i))/dx2;
   else
               dcdx=(c(i+1)-c(i))/dx
               dcdx2=(c(i-1)-2*c(i)+c(i+1))/dx2;
               ct(i)=d*dcdx2-us*dcdx;


   end
```

```
    end
  ct=ct';
```

the number of ODEs (n) is determined by the command *n=length(c)*. The finite difference interval (*dx*) and its square (*dx2*) is then computed. The specification of the solid velocity (*us*) and the diffusion coefficient (*d*) take values from literature.
The MOL programming of the n ODEs is done in the for loop. For Boundary Condition (4.7), the coding is

```
    if(i==1)    ct(i)=0;
```

For BC (4.8), the coding is

```
elseif(i==n) ct(i)=d*(c(i-1)-c(i))/dx2;
```

From this line of code it is important to note that the fictitious value *c(n+1)* has been replaced by *c(n)* in the ODE specification.
For the remaining interior points the programming is

```
else
    dcdx=(c(i+1)-c(i))/dx
    dcdx2=(c(i-1)-2*c(i)+c(i+1))/dx2;
    ct(i)=d*dcdx2-us*dcdx;
```

Which follows from the Finite Difference approximation of the axial dispersion model (eq. (4.4)).

Since the Matlab ODE integrators require a column vector of derivatives, a final transpose of ut is required.

```
  ct=ct';
  ncall=ncall+1;
```

Finally, the number of calls to the sub-routine is incremented so that at the end of the solution, the value of ncall displayed by the main program gives an indication of the computational effort required to produce the entire solution.

5.2 Evaluation of the RTD

The selected parameter for the description of the RTD is the residence time distribution function $E(t)$ eq.(3.10). This function has been represented by a row vector having a number of elements equal to the number of lines chosen for the evaluation of the ADM. $E(t)$ is evaluated using some additional command lines in the main MatLab code.

```
lastcolumn=c(:,n);
integral=0;
```

```
for index=1:n
    integral=c(index,n)*(1/n)+integral;
end
E=lastcolumn/integral
figure(4);
  x3=linspace(0,1,n);
  y3=E;
  plot(x3,y3,'linestyle','-','linewidth',4)
check=0;
for i=1:n
    check=E(i)*(1/n)+check;
end
```

$C(t)$ corresponds to $c(t,z)$ evaluated at $z = L$, this means that it is nothing else that the last column of the concentration matrix c.

```
lastcolumn=c(:,n);
```

Evaluation of $\int_0^\infty C(t)dt$ means to compute the integral of the curve that we obtain at the exit of the reactor (Figure 5). $E(t)$ can be then evaluated and plotted.

```
integral=0;
for index=1:n
    integral=c(index,n)*(1/n)+integral;
end
E=lastcolumn/integral
figure(4);
  x3=linspace(0,1,n);
  y3=E;
  plot(x3,y3,'linestyle','-','linewidth',4)
```

The plot has the same shape of the curve obtained at $z = L$ since the residence time distrubution function is just the normalization of the tracer concentration that leaves the reactor at time t. As a consequence, it is expected that the integral over the time domain of $E(t)$ has a unitary value, being $E(t)$ a Gaussian curve.

```
check=0;
for i=1:n
    check=E(i)*(1/n)+check;
end
```

5.2.1 **Evaluation of the RTD in function of the mean travelling velocity**

Up to now, in the evaluation of the Residence Time Distribution function $E(t)$, time was considered as the computation independent variable.

The next step connects the result of this work with what has already been done in the study of the energy balance in a fast pyrolysis screw reactor. Such study uses as input parameters an arbitrary number of velocity characteristics of the exit concentration, i.e. a sequence of values of the Residence Time Distribution in function of the exit velocity $E(v)$. This means that $E(v)$ should be evaluated where v is the mean velocity of a specific tracer concentration. Therefore, the domain of the RTD function should be changed. The reasoning that has been done refers to figure 8.
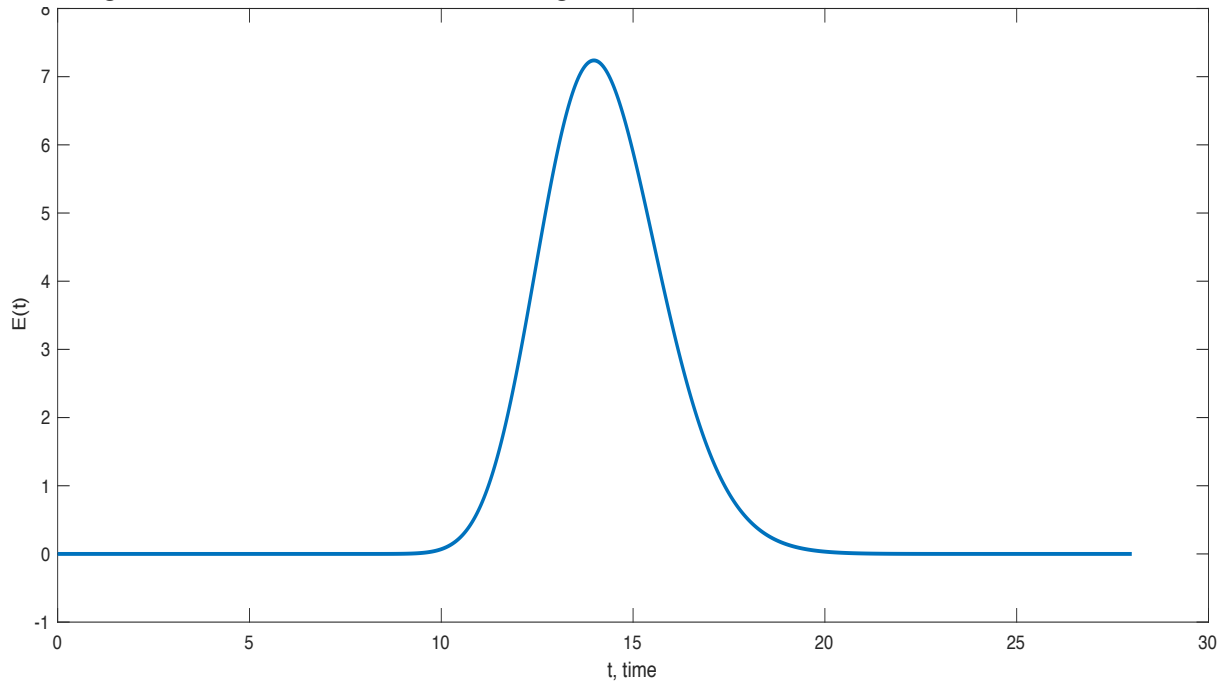
Figure 8: plot of the Residence Time Distribution function

Considering an arbitrary value of $E(t)$, the time after which that specific concentration has left the reactor is specified. Since the reactor has a fixed length, the average velocity with which the concentration has travelled can be calculated as well. However, for each concentration, there exist two distinct values of time and, as a consequence, two different velocities. The higher velocity will be the one corresponding to the lower time and, on the other side, the lower velocity will be the one associated with the greater time. This means that, to express $E(t)$ in function of the velocity, it can be noted that, for a specific concentration E, we have t_a, t_b, v_a, v_b with $t_b > t_a$ and $v_a > v_b$. Therefore, $E(t_a) = E(v_b)$ and $E(t_b) = E(v_a)$.

All of this translates in building the vector $E(v)$ by considering the ith element of $E(v)$ equal to the $(n-1+i)^{th}$ element of $E(t)$, where n is the length of $E(t)$ (equal to the number of lines chosen for the computation).

To evaluate this, the following lines of code allow the computation of the velocity distribution and its resampled form:

```
Ev=E;
for index=1:n
    Ev(index)=E(n+1-index);
end
```

The obtained vector will have a number of values equal to the number of lines initially chosen. In order to obtain a reslut which may be directly inserted in the code for the energy balance, a resample of $E(v)$ is needed. Moreover, the number of resampled points should be arbitrarily chosen by the user. This means to translate the continuous function $E(v)$ into a step function where the number of steps can be decided.
This has been done using the following code lines:

```
r=50; %amount of resamples
f=n/r; %resampling interval
q=zeros(1,r);
for index=1:r
    q(index)=Ev(index*f);
end
k=zeros(1,n);
for j=1:r
    if j==1
        for i=1:n
            k(i)=q(j);
        end
    else
        for index=((j-1)*f+f/2):n
            k(index)=q(j);
        end
    end
end
figure(5);
  x4=linspace(0,1,n);
  y4=Ev;
  x5=linspace(0,1,n);
  y5=k;
  plot(x4,y4,x5,y5,'linestyle','-','linewidth',4)
  title('plot of E(v) and its resampling')
  xlabel('time')
  ylabel('Ev (blue), k (red)')

%check resampled area
   check2=0;
for i=1:n
    check2=k(i)*(1/n)+check2;
end
```

Some comments about this code are mandatory. Initially, the number of resampling points is determined and the resampling interval is calculated

```
r=50; %amount of resamples
f=n/r; %resampling interval
```

A vector having length equal to the number of resamples with the corresponding values of $E(v)$ is then builted

```
q=zeros(1,r);
for index=1:r
    q(index)=Ev(index*f);
end
```

Finally, the vector representing the step function having as values the resampled ones and that can be inserted directly in the matrix for the energy balance computation, is builted

```
k=zeros(1,n);
for j=1:r
    if j==1
        for i=1:n
            k(i)=q(j);
        end
    else
        for index=((j-1)*f+f/2):n
            k(index)=q(j);
        end
    end
end
```

Essentially, this code creates a vector of *n* elements (*k*) starting from a vector of *r* elements (*q*) with *n>r*. Values are assigned to *k* for each resampling interval and the assigned values are taken from the vector *q*. In this way the vector *k* will be formed by "packages" of values equal to the values of *q*. *k* will therefore represent our step function. A plot is made to visualize the continuous function $E(v)$ and its resampled form

```
figure(5);
  x4=linspace(0,1,n);
  y4=Ev;
  x5=linspace(0,1,n);
  y5=k;
  plot(x4,y4,x5,y5,'linestyle','-','linewidth',4)
  title('plot of E(v) and its resampling')
  xlabel('time')
  ylabel('Ev (blue), k (red)')
```

It is important to note that, if all the calculations have been done in a correct way, the area of the step function must be equal to one since it is always a representation of the Residence Time Distribution function and, therefore, must satisfy the gaussian condition of unitary area. As usual, an easy check may be built in the main program.

```
%check resampled area
```

```
    check2=0;
for i=1:n
    check2=k(i)*(1/n)+check2;
end
```

Concludig, we can observe that the numerical evaluation of the RTD has shown results in coherence with the 3-D DEM simulation. A distribution of the particle's velocities inside the reactor have been obtained. The final step is the collection of the results and the evaluation of a parametric analysis.

6.Analysis of Results

Results obtained from the Matlab code are here analyzed. A parametric analysis of the ADM has been done to understand how the different parameters influence the distribution of the tracer inside the reactor. Moreover, the $E(v)$ continuous distribution can be used in a resampled shape. The latter is the final result of this thesis project, the one that must be integrated into the previously made studies about the pyrolyzer operating framework.

6.1 Parametric analysis of the Axial Dispersion Model

Once the ADM is solved by means of the MOL, can be noticed as the main parameters influencing the distribution of the concentration are: the solid velocity u_s, the diffusion coefficient D_{ax} and the chosen number of lines n for the MOL evaluation.
The influence of these parameters on the final solution is fundamental to understand how the operating parameters can be properly selected to optimize the particles distribution inside the reactor.
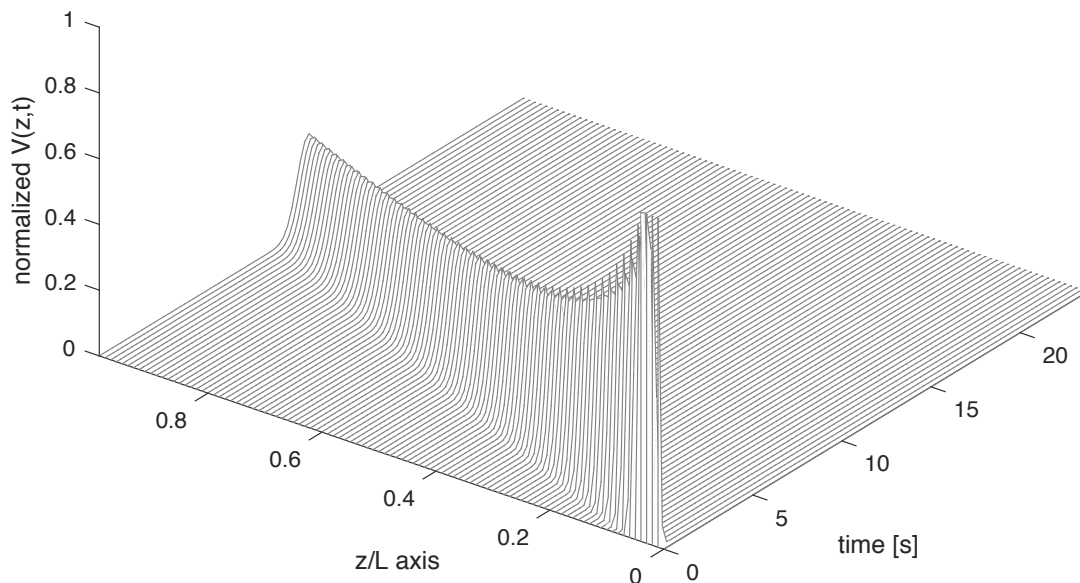

Figure 9: ADM solution

6.1.1 Influence of the solid velocity us

By keeping constant both the number of lines (n=620) and the diffusion coefficient (D_{ax} =10^{-5}), can be observed a profile variation decreasing the solid velocity u_s.
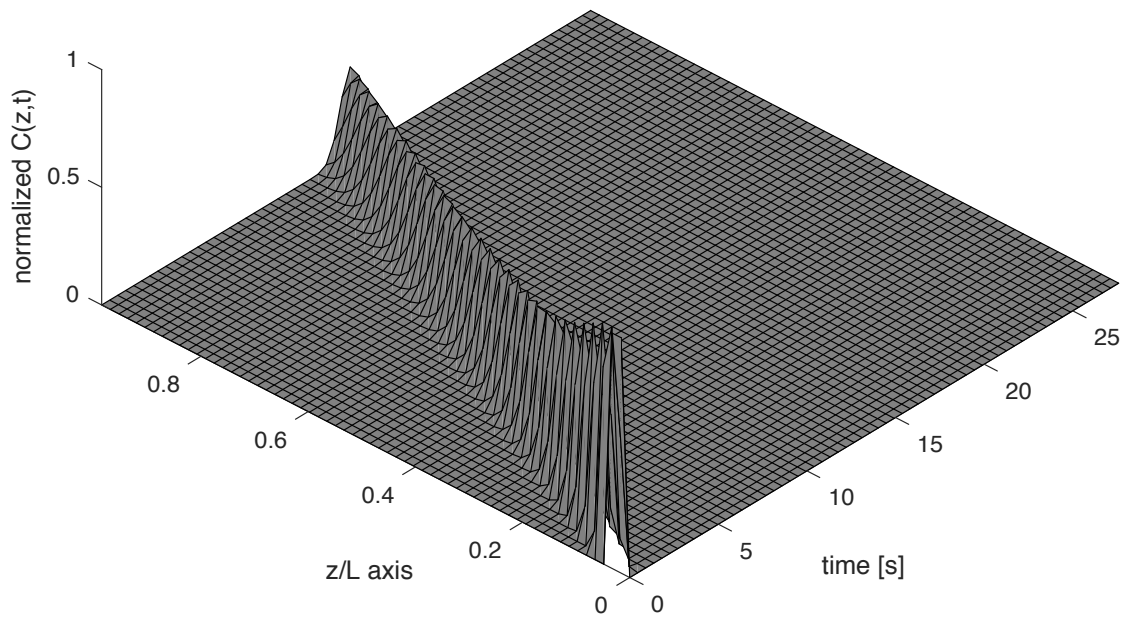
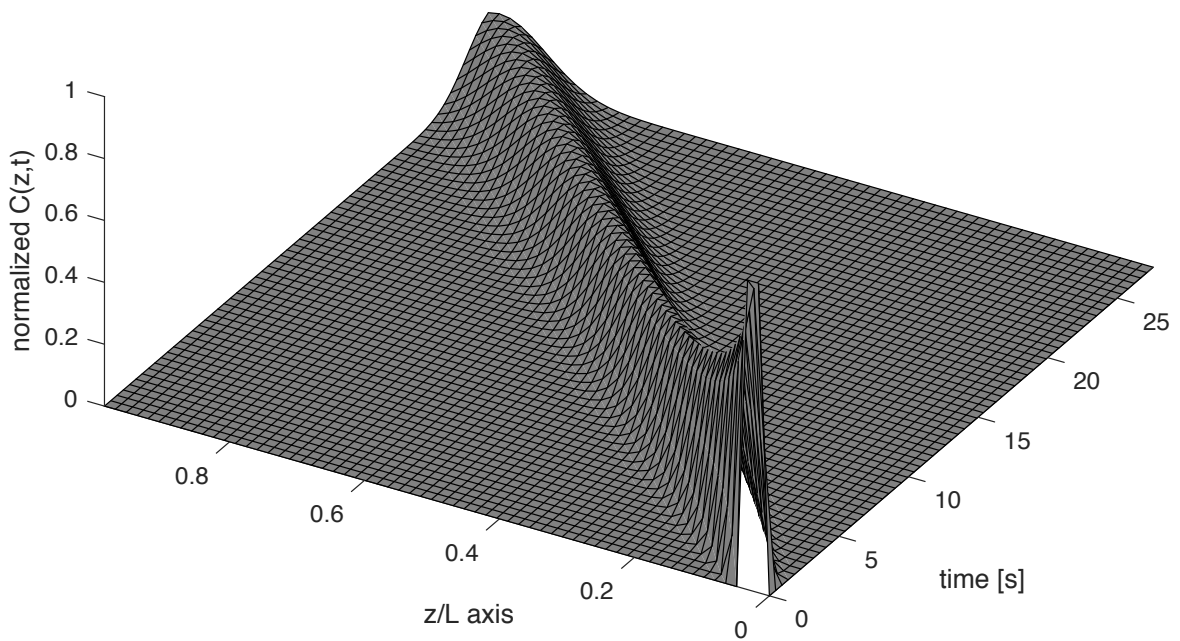*Figure 10: Fokker Plank Equation – MOL Solution us=0.0206*

Figure 11: Fokker Plank Equation – MOL Solution us=0.0103

In this example the solid velocity has been decreased by the 50% of the original value.
It is immediate to note that there are two main results in changing this parameter. The first one is that the time required for the tracer to reach the end of the reactor (z/L=1) increased relevantly, passing approximately from 11 to 22 seconds. The second result is that the convexity of the curve has changed being the one for u_s=0.0103 more flat than the one for u_s=0.0206. This results are relevant in the design of the reactor characteristics. Clearly, the time required for the particles to exit the reactor is an important parameter since it will change considerably the heating histories of the different particles. An higher time means that the reaction to which they are subjected will last long. This should be properly modeled to obtain the desired result. The reference value u_s=0.0206 gives exit times of the order of 11 seconds. This is in line with a fast pyrolysis process where the time for the reactions are considered to be around 5 seconds, which Is the required time for half reactor. The variation in the curve convexity must be considered as well. In fact, as will be better explained when considering the variation of the diffusion coefficient, an higher convexity means a lower uniformity of the different reactions. Again, u_s=0.0206 has given good result under this point of view.

6.1.2 Influence of the diffusion coefficient D_{ax}

The influence of the diffusion coefficient in the overall result can be observed keeping the number of lines n=620 and the solid velocity u_s=0.0206.
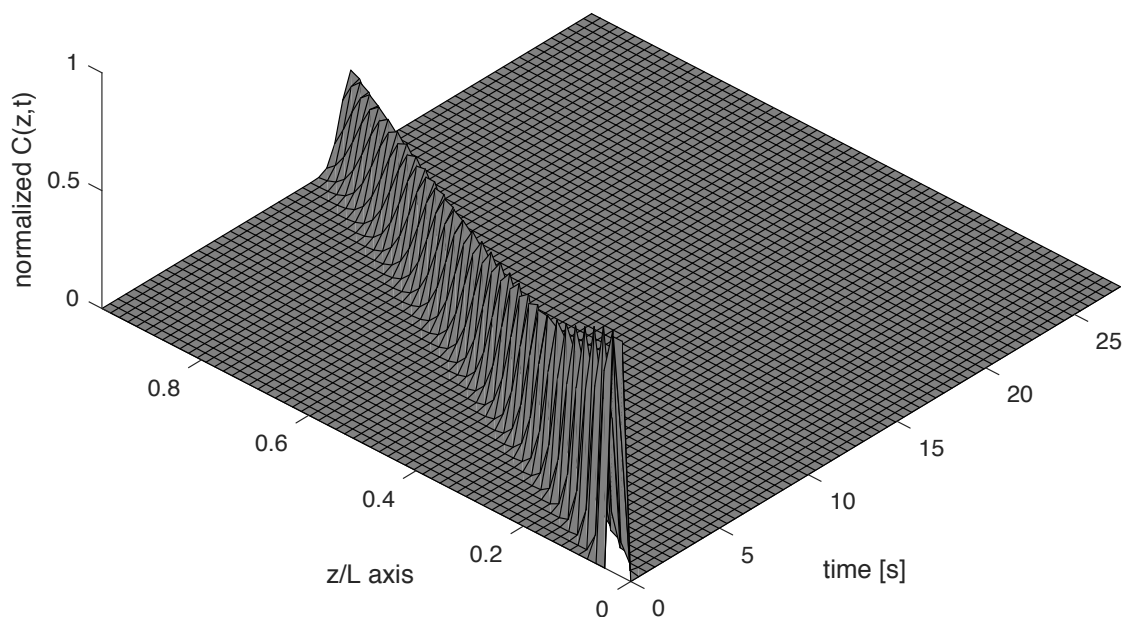Results are highlithed for D_{ax} =10^{-5} and D_{ax} =$3 \cdot 10^{-5}$

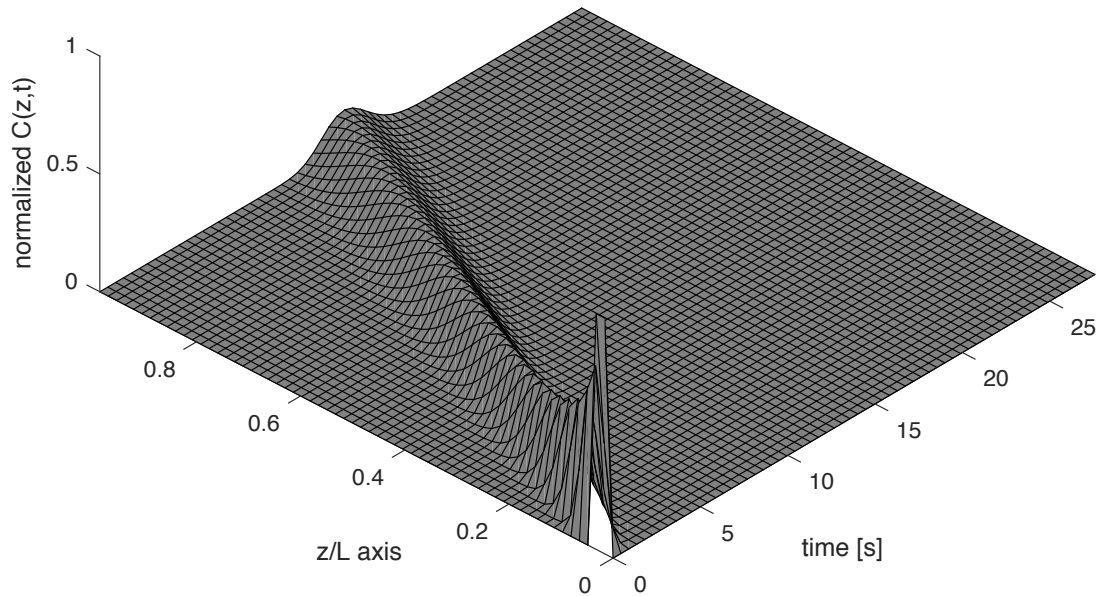*Figure 12: Fokker Plank Equation – MOL Solution d=0.00001*

Figure 13: Fokker Plank Equation – MOL Solution d=0.00003

Increasing the diffusion coefficient of the 300% can be noted that the distribution of the tracer happens in a faster way. This is translated in a steeper curve after the tracer injection and in the increase in the convexity of the plot over the entire space domain. In this case, the increase of the diffusion coefficient has no effect on the average time required for the tracer to reach the end of the reactor. The convexity of the curve is an important aspect to consider in this evaluation. An higher convexity means that the RTD of the different particle will be less uniform. This is translated into very different heating histories for the different fractions. As a consequence, the reactions to which the different particles are subjected in the process, are predicted to vary more as we increase the diffusion coefficient. This suggest to keep the coefficient D_{ax} as low as possible in order to have uniform reactions for the different particles inside the reactor.

6.1.3 **Influence of the lines number *n***

The choice of the number of lines used for the MOL will determine the number of ODEs solved by the code. This means that a change in the number of lines will change significantly the computational effort. The time required for the solution of the PDE will increase as *n* increases, but the reward will be a solution which better approximates the analytical one.
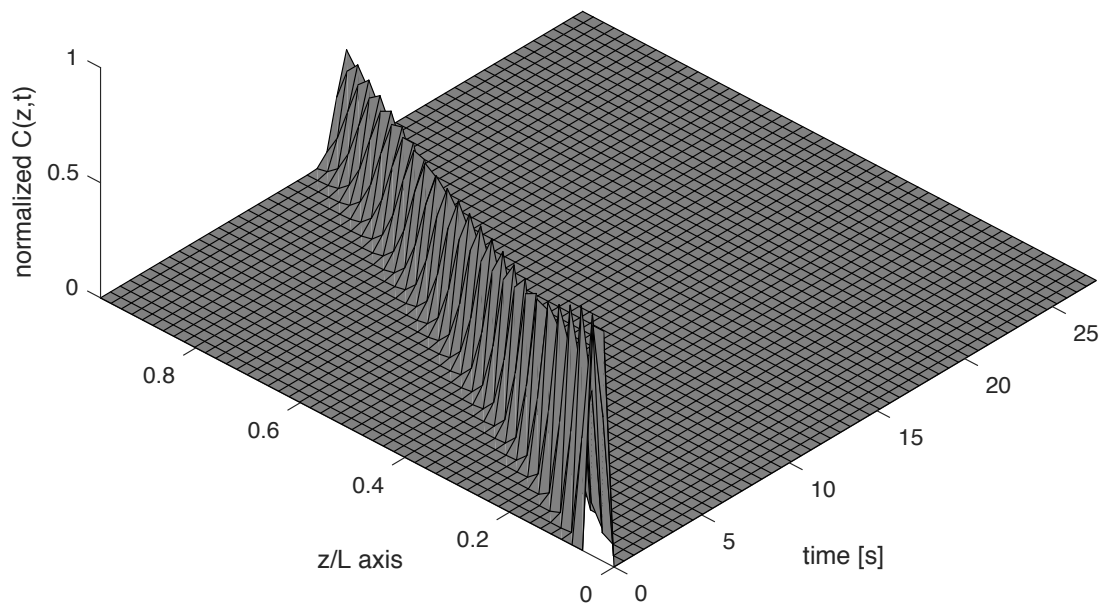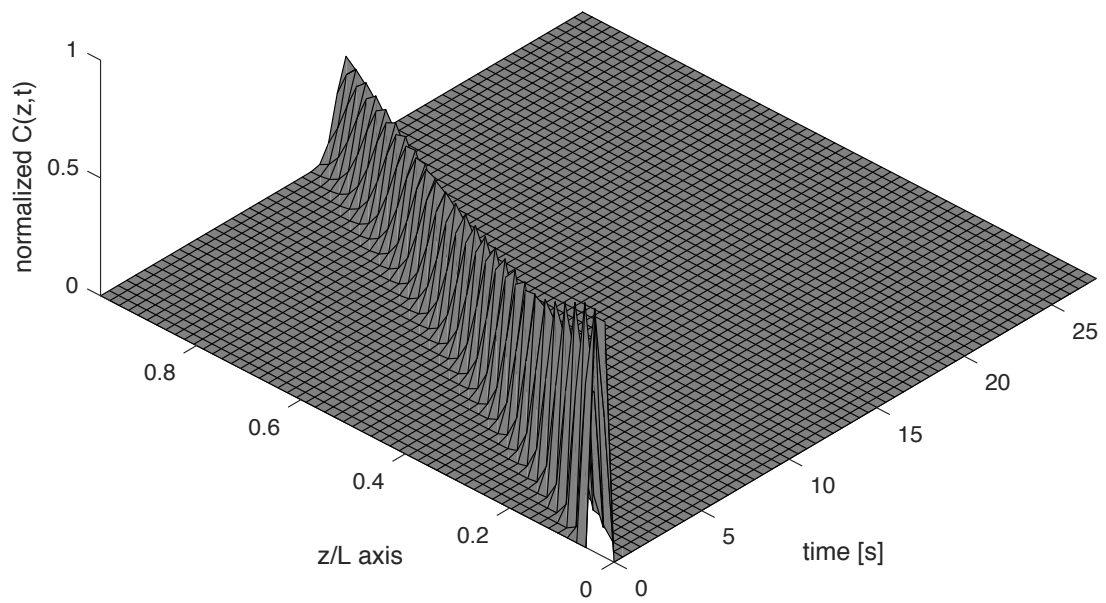
Figure 14: Fokker Planck Equation - MOL solution n=500
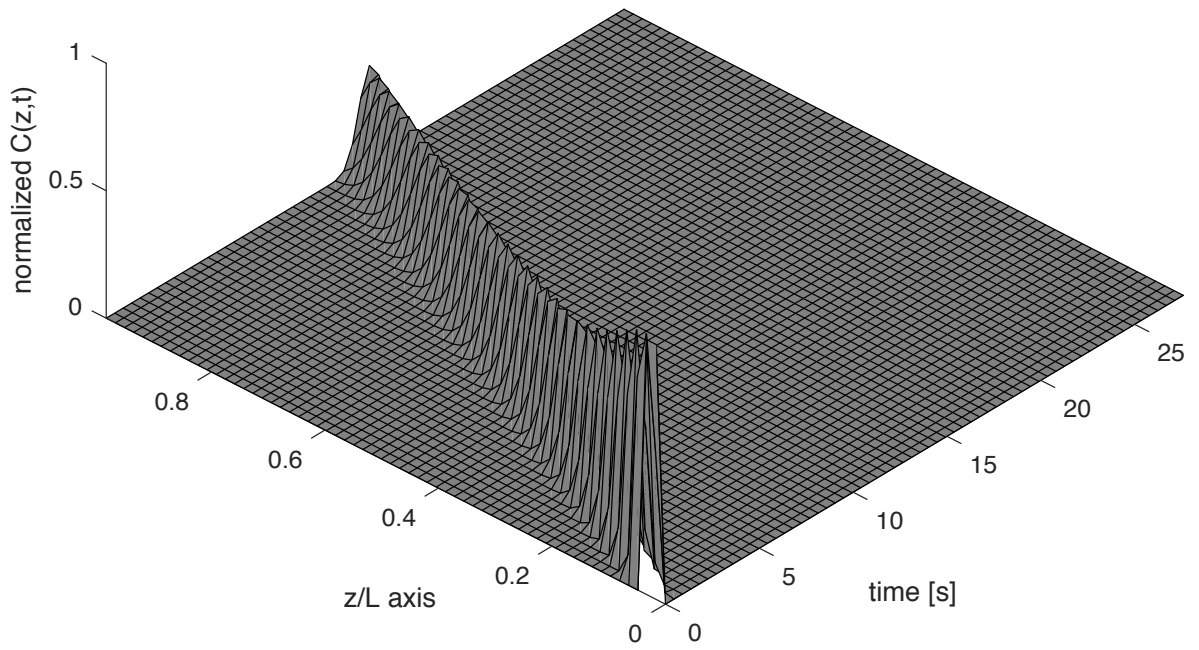

Figure 15: Fokker Planck Equation - MOL solution n=560

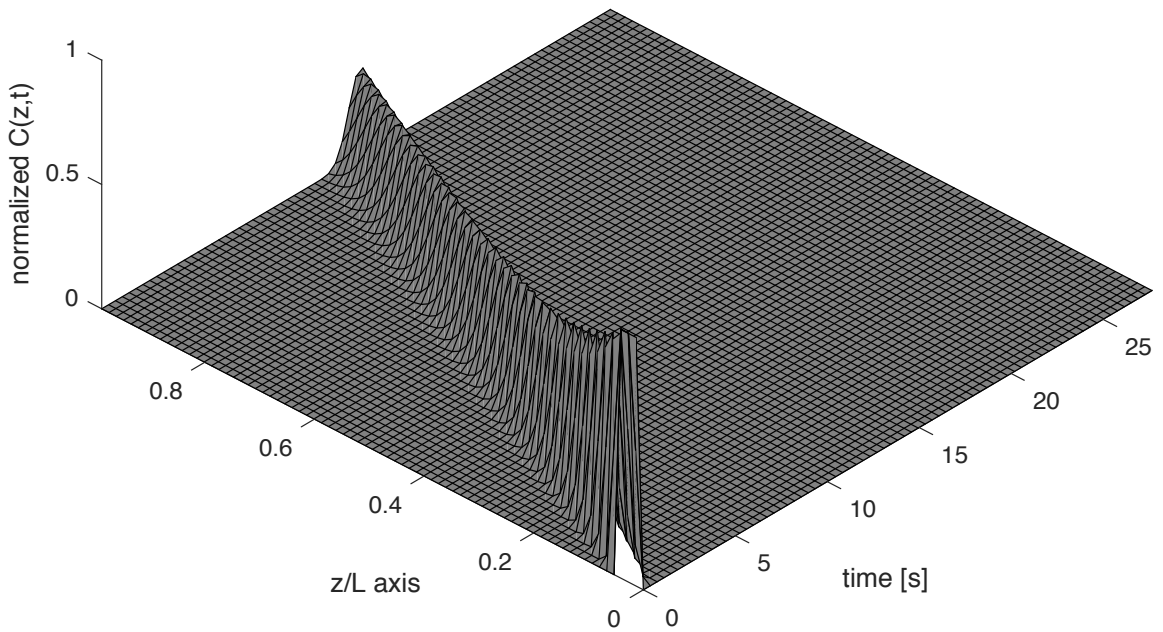*Figure 16: Fokker Planck Equation - MOL solution n=620*

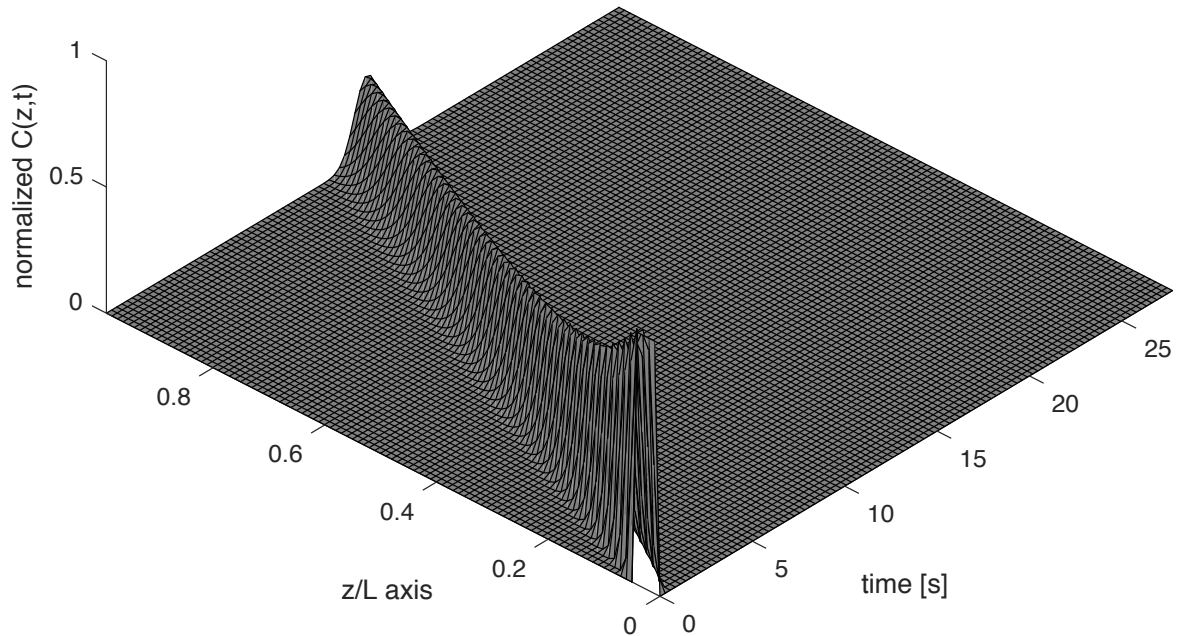*Figure 17: Fokker Planck Equation - MOL solution n=750*

Figure 18: Fokker Planck Equation - MOL solution n=1000

It can be immediately observed that the grid over which the plot is computed is more dense as we increase the number of lines ***n***. However, the major result in increasing this parameter is the decrease in the numerical diffusion. As a consequence, the error propagation will be decreased as well. The result will be a simulation which better approximate the real behavior of the RTD in a screw conveyor. In fact, the quantity of tracer detected at a specific time instant will be closer to the amount of injected tracer. The resulting Gaussian curve at the exit of the reactor $(x/l = 1)$ is also influenced by the choice of the number of lines. In fact, as it increases, the shape of the curve will change, becoming more flat. It should be noted, however, that the decrease of the error in the measurement has been observed just for ***n***<620. For this value, the measured relative error at two different time instants was on the order of 0.65%. In fact, for ***n***>620, an inversion of the trend was present with consequent increase in the resulting error as ***n*** was increased. The reason for this behavior has to be referred to PDE discretization method. In particular, on the selection of a forward Finite Difference approximation in the Fokker Planck Equation.

6.2 $E(v)$ Resampling

It has been previously observed that, the time domain of the Residence Time Distribution can be converted into a velocity domain once the reactor length is specified. In this case again, the velocity distribution curve shape is expected to be again a Gaussian curve as

the one obtained for $E(t)$. Together with the plot of $E(v)$ it is interesting to show also its resampled form so that to have an overview about how they are connected.
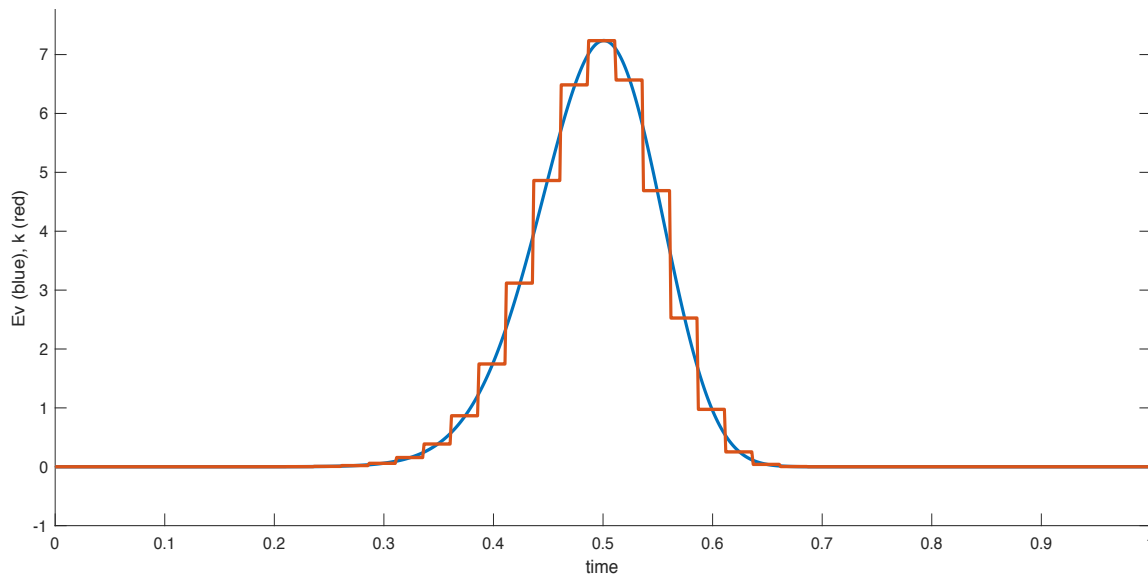

Figure 19: plot of E(v) and its resampling

As said before, resampling $E(v)$ is fundamental to obtain a finite number of values to insert into the heat transfer model of the fast pyrolysis process.

As expected, the resampled form of $E(v)$ (k in figure 16) will be a step function with the specified resampling interval. In this way, instead of a continuous function with an infinite number of values for $E(v)$, another function can be considered. This one with a finite number of values to be decided arbitrarily. This gives the possibility of inserting it inside the energy balance matrix. The resampling interval must be chosen coherently with the dimensions of the matrix describing the heat transfer.

7.Conclusions

In this project thesis, the particles Residence Time Distribution inside a screw reactor has been obtained by numerical solution of an Axial Dispersion Model. A MatLab code has been developed to solve the convective-diffusive Axial Dispersion Model partial differential equation into a number of arbitrarily chosen ODE. The system has been subsequently solved with the use of the MatLab integrator ode15s. The main obtained results are the following:

- The Axial Dispersion Model has been solved through a numerical evaluation by means of the Method Of Lines. In particular, the finite difference approximations of the space derivatives has been considered to build a system of ODEs with time as the independent variable. Initial and boundary conditions have been specified to complete the description of the PDE problem. Finally, the system has been solved in MatLab environment.

- A parametric analysis of the ADM has been performed on the main parameters in the Fokker-Planck equation, namely, the number of lines, the diffusion coefficient and the solid velocity. In particular, it has been observed that decreasing the solid velocity, as well as increasing the diffusion coefficient, will increase the convexity of the curve. Consequently, the RTD of the different particle will be less uniform. Moreover, increasing the number of lines, the solution will better approximate the real RTD in a screw conveyor since the numerical diffusion of the error will decrease.

- Residence time and velocity distribution of mass particles inside the reactor of a fast pyrolysis process has been evaluated.

As a final result, the distribution can be coupled with a comprehensive heat and mass transfer code developed for fast pyrolysis purposes.

8.Bibliography

1.   Wang, J., et al., *Review and prospect of integrated demand response in the multi-energy system.* Applied Energy, 2017.
2.   Su, Q., W. Yang, and Y. Liu, *Optimization of carbon emission considering production planning at enterprise level.* Journal of Cleaner Production, 2017. **162**: p. 635-645.
3.   Zaman, K. and M.A.-e. Moemen, *Energy consumption, carbon dioxide emissions and economic development: Evaluating alternative and plausible environmental hypothesis for sustainable growth.* Renewable and Sustainable Energy Reviews, 2017. **74**: p. 1119-1130.
4.   Fortes, P., et al., *Integrated technological-economic modeling platform for energy and climate policy analysis.* Energy, 2014. **73**: p. 716-730.
5.   Kung, C.-C. and N. Zhang, *Renewable energy from pyrolysis using crops and agricultural residuals: An economic and environmental evaluation.* Energy, 2015. **90, Part 2**: p. 1532-1544.
6.   Cordiner, S., et al., *Fuel cell based Hybrid Renewable Energy Systems for off-grid telecom stations: Data analysis from on field demonstration tests.* Applied Energy, 2016.
7.   Bhattacharya, M., et al., *The effect of renewable energy consumption on economic growth: Evidence from top 38 countries.* Applied Energy, 2016. **162**: p. 733-741.
8.   Reuter, W.H., et al., *Renewable energy investment: Policy and market impacts.* Applied Energy, 2012. **97**: p. 249-254.
9.   Inglesi-Lotz, R., *The impact of renewable energy consumption to economic growth: a panel data application.* Energy Economics, 2016. **53**: p. 58-63.
10.   Adewuyi, A.O. and O.B. Awodumi, *Biomass energy consumption, economic growth and carbon emissions: Fresh evidence from West Africa using a simultaneous equation model.* Energy, 2017. **119**: p. 453-471.
11.   Zhang, F., et al., *Cost, energy use and GHG emissions for forest biomass harvesting operations.* Energy, 2016. **114**: p. 1053-1062.
12.   Bhutto, A.W., et al., *Insight into progress in pre-treatment of lignocellulosic biomass.* Energy, 2017.
13.   Nam, H., et al., *Experimental investigation of pyrolysis of rice straw using bench-scale auger, batch and fluidized bed reactors.* Energy, 2015. **93**: p. 2384-2394.
14.   Cordiner S , M.A., Mulone V, Rocco V, *Biomass pyrolysis modeling of systems at laboratory scale.* International Journal of Numerical Methods for Heat and Fluid Flow, 2017.
15.   Plis, P. and R. Wilk, *Theoretical and experimental investigation of biomass gasification process in a fixed bed gasifier.* Energy, 2011. **36**(6): p. 3838-3845.
16.   Aysu, T. and M.M. Küçük, *Biomass pyrolysis in a fixed-bed reactor: Effects of pyrolysis parameters on product yields and characterization of products.* Energy, 2014. **64**: p. 1002-1025.
17.   Huang, Y.-F., et al., *Microwave pyrolysis of lignocellulosic biomass: Heating performance and reaction kinetics.* Energy, 2016. **100**: p. 137-144.
18.   Oh, S.-J., G.-G. Choi, and J.-S. Kim, *Characteristics of bio-oil from the pyrolysis of palm kernel shell in a newly developed two-stage pyrolyzer.* Energy, 2016. **113**: p. 108-115.
19.   Kim, J.-Y., et al., *Assessment of miscanthus biomass (Miscanthus sacchariflorus) for conversion and utilization of bio-oil by fluidized bed type fast pyrolysis.* Energy, 2014. **76**: p. 284-291.
20.   Humbird, D., et al., *One-Dimensional Biomass Fast Pyrolysis Model with Reaction Kinetics Integrated in an Aspen Plus Biorefinery Process Model.* ACS Sustainable Chemistry & Engineering, 2017.
21.   Pattiya, A., S. Sukkasi, and V. Goodwin, *Fast pyrolysis of sugarcane and cassava residues in a free-fall reactor.* Energy, 2012. **44**(1): p. 1067-1077.
22.   Quek, A. and R. Balasubramanian, *Mathematical modeling of rubber tire pyrolysis.* Journal of Analytical and Applied Pyrolysis, 2012. **95**: p. 1-13.

23. Cordiner, S., et al., *A detailed study of a multi-MW biomass combustor by numerical analysis: evaluation of fuel characteristics impact.* Energy Procedia, 2014. **61**: p. 751-755.

24. Cordiner, S., et al., *Biomass furnace study via 3D numerical modeling.* International Journal of Numerical Methods for Heat & Fluid Flow, 2016. **26**(2): p. 515-533.

25. Park, C., et al., *Effect of process operating conditions in the biomass torrefaction: A simulation study using one-dimensional reactor and process model.* Energy, 2015. **79**: p. 127-139.

26. Peduzzi, E., et al., *Torrefaction modelling for lignocellulosic biomass conversion processes.* Energy, 2014. **70**: p. 58-67.

27. Baruah, D. and D. Baruah, *Modeling of biomass gasification: a review.* Renewable and Sustainable Energy Reviews, 2014. **39**: p. 806-815.

28. Martínez-Lera, S. and J.P. Ranz, *On the development of a wood gasification modelling approach with special emphasis on primary devolatilization and tar formation and destruction phenomena.* Energy, 2016. **113**: p. 643-652.

29. Chaurasia, A., *Modeling, simulation and optimization of downdraft gasifier: Studies on chemical kinetics and operating conditions on the performance of the biomass gasification process.* Energy, 2016. **116**: p. 1065-1076.

30. Patra, T.K., K. Nimisha, and P.N. Sheth, *A comprehensive dynamic model for downdraft gasifier using heat and mass transport coupled with reaction kinetics.* Energy, 2016. **116**: p. 1230-1242.

31. Papari, S. and K. Hawboldt, *A review on the pyrolysis of woody biomass to bio-oil: Focus on kinetic models.* Renewable and Sustainable Energy Reviews, 2015. **52**: p. 1580-1595.

32. Jeong, J.-Y., et al., *Production of bio-oil rich in acetic acid and phenol from fast pyrolysis of palm residues using a fluidized bed reactor: Influence of activated carbons.* Bioresource Technology, 2016. **219**: p. 357-364.

33. Lam, S.S., et al., *Progress in waste oil to sustainable energy, with emphasis on pyrolysis techniques.* Renewable and Sustainable Energy Reviews, 2016. **53**: p. 741-753.

34. Di Blasi, C., *Modeling chemical and physical processes of wood and biomass pyrolysis.* Progress in Energy and Combustion Science, 2008. **34**(1): p. 47-90.

35. Bridgwater, A. and G. Peacocke, *Fast pyrolysis processes for biomass.* Renewable and sustainable energy reviews, 2000. **4**(1): p. 1-73.

36. Bridgwater, A.V., *Review of fast pyrolysis of biomass and product upgrading.* Biomass and bioenergy, 2012. **38**: p. 68-94.

37. Aramideh, S., et al., *Numerical simulation of biomass fast pyrolysis in an auger reactor.* Fuel, 2015. **156**: p. 234-242.

38. Funke, A., et al., *Dimensional Analysis of Auger-Type Fast Pyrolysis Reactors.* Energy Technology, 2017. **5**(1): p. 119-129.

39. Fogler, H.S., *Elements of chemical reaction engineering.* 1999.

40. Gao, Y., F.J. Muzzio, and M.G. Ierapetritou, *A review of the Residence Time Distribution (RTD) applications in solid unit operations.* Powder Technology, 2012. **228**: p. 416-423.

41. Hamdi, S., W.E. Schiesser, and G.W. Griffiths, *Method of lines.* Scholarpedia, 2007. **2**(7): p. 2859.

42. Luz, F.C., et al. *Fast pyrolysis in a shaftless screw reactor: a 1-d numerical model.* in *SEEP2017.* 2017. Bled,Slovenia.

43. Luz, F.C., et al. *Biomass fast pyrolysis process at laboratory scale:residence time and heating up evaluation in a shaftless screw reactor by means of a discrete element model approach.* in *CHT-17.* 2017. Naples.

44. Li, S.Q., et al., *A Mathematical Model of Heat Transfer in a Rotary Kiln Thermo-Reactor.* Chemical engineering & technology, 2005. **28**(12): p. 1480-1489.

45. Gorog, J., J. Brimacombe, and T. Adams, *Radiative heat transfer in rotary kilns.* Metallurgical Transactions B, 1981. **12**(1): p. 55-70.

46. Wes, G., A.A. Drinkenburg, and S. Stemerding, *Heat transfer in a horizontal rotary drum reactor.* Powder Technology, 1976. **13**(2): p. 185-192.

47. Tscheng, S. and A. Watkinson, *Convective heat transfer in a rotary kiln.* The Canadian Journal of Chemical Engineering, 1979. **57**(4): p. 433-443.

48.   Babler, M.U., et al., *Modeling and pilot plant runs of slow biomass pyrolysis in a rotary kiln.* Applied Energy.

49.   Nwabueze, T.U. and M.O. Iwe, *Residence Time Distribution (RTD) in a Single Screw Extrusion of African Breadfruit Mixtures.* Food and Bioprocess Technology, 2008. **3**(1): p. 135.

50.   Sisay, M.T., et al., *Residence time distribution and flow pattern of reduced-gluten wheat-based formulations in a twin–screw extruder.* LWT - Food Science and Technology, 2017. **79**: p. 213-222.

51.   Huo, C., et al., *Residence Time Distribution of Particles in a Screw Feeder: Experimental and Modelling Study.* The Canadian Journal of Chemical Engineering, 2015. **93**(9): p. 1635-1642.

52.   Nachenius, R.W., et al., *Residence time distributions of coarse biomass particles in a screw conveyor reactor.* Fuel Processing Technology, 2015. **130**: p. 87-95.

53.   Rastegar, S.O. and T. Gu, *Empirical correlations for axial dispersion coefficient and Peclet number in fixed-bed columns.* Journal of Chromatography A, 2017. **1490**: p. 133-137.

54.   Sievers, D.A., et al., *Online residence time distribution measurement of thermochemical biomass pretreatment reactors.* Chemical Engineering Science, 2016. **140**: p. 330-336.